Diffusion-Weighted MRI of Breast Cancer: Improved Lesion Visibility and Image Quality Using Synthetic b-Values

Hubert Bickel, MD,[1] Stephan H. Polanec, PhD,[1] Georg Wengert, PhD,[1]
Katja Pinker, PhD,[1,2] Wolfgang Bogner, PhD,[3] Thomas H. Helbich, MD,[1] and
Pascal A. Baltzer, MD[1]*

Background: Diffusion-weighted imaging (DWI) is an MRI technique with the potential to serve as an unenhanced breast cancer detection tool. Synthetic b-values produce images with high diffusion weighting to suppress residual background signal, while avoiding additional measurement times and reducing artifacts.

Purpose: To compare acquired DWI images (at b = 850 s/mm^2) and different synthetic b-values (at b = 1000–2000 s/mm^2) in terms of lesion visibility, image quality, and tumor-to-tissue contrast in patients with malignant breast tumors.

Study Type: Retrospective.

Population: Fifty-three females with malignant breast lesions.

Field Strength/Sequence: T$_2$w, DWI EPI with STIR fat-suppression, and dynamic contrast-enhanced T$_1$w at 3T.

Assessment: From acquired images using b-values of 50 and 850 s/mm^2, synthetic images were calculated at b = 1000, 1200, 1400, 1600, 1800, and 2000 s/mm^2. Four readers independently rated image quality, lesion visibility, preferred b-value, as well as the lowest and highest b-value, over the range of b-values tested, to provide a diagnostic image.

Statistical Tests: Medians and mean ranks were calculated and compared using the Friedman test and Wilcoxon signed-rank test. Reproducibility was analyzed by intraclass correlation (ICC), Fleiss, and Cohen's κ.

Results: Relative signal-to-noise and contrast-to-noise ratios decreased with increasing b-values, while the signal-intensity ratio between tumor and tissue increased significantly ($P < 0.001$). Intermediate b-values (1200–1800 s/mm^2) were rated best concerning image quality and lesion visibility; the preferred b-value mostly lay at 1200–1600 s/mm^2. Lowest and highest acceptable b-values were 850 s/mm^2 and 2000 s/mm^2. Interreader agreement was moderate to high concerning image quality (ICC: 0.50–0.67) and lesion visibility (0.70–0.93), but poor concerning preferred and acceptable b-values (κ = 0.032–0.446).

Data Conclusion: Synthetically increased b-values may be a way to improve tumor-to-tissue contrast, lesion visibility, and image quality of breast DWI, while avoiding the disadvantages of performing DWI at very high b-values.

Level of Evidence: 3

Technical Efficacy: Stage 2

DYNAMIC CONTRAST-ENHANCED magnetic resonance imaging (MRI) of the breast is the most sensitive test for breast cancer detection and is recommended for several indications, including screening of women at intermediate (>15%)[1] and high (>20%)[2–4] risk of breast cancer. However, with the recent concerns about the safety of gadolinium-containing contrast agents,[5,6] there are considerable efforts to develop unenhanced MRI techniques with equal sensitivity for breast MRI. In this context, diffusion-weighted imaging (DWI)

has been recognized as a robust, reliable, and fast MRI sequence[7–9] that has the potential to fulfill the need for an unenhanced technique for breast cancer screening. DWI measures the random movement of water molecules, and the intensity of diffusion weighting is described by the b-value. Ideally, on very high b-value images, only structures with both high water signal and high diffusion restriction, such as most malignant breast tumors, should remain visible. However, higher applied b-values lead to an increase of imaging artifacts, image

noise,[10] and decreased signal-to-noise ratio (SNR), requiring prolonged measurement times. Therefore, the b-values applied in practice are usually a compromise between diffusion weighting and image noise.[11]

This compromise could be partially overcome using synthetic b-values: In a monoexponential diffusion model, the signal decrease in increasing b-values is theoretically logarithmic. Therefore, images for every possible b-value can be mathematically calculated from two DWI acquisitions with different b-values. With these calculated images, it should be possible to avoid the increase in eddy current artifacts and the risk of movement artifacts coming with increased b-values and prolonged measurement times. While this topic has been more extensively investigated in the prostate,[12–17] data are scarce concerning the breast,[18,19] where the optimal synthetic b-value for the detection of malignant breast tumors remains unclear.

Therefore, the aim of this study was to evaluate whether synthetically increased b-values would provide an advantage over breast DWI using commonly acquired b-values, and which synthetic b-value would perform best in terms of general image quality and lesion visibility in patients with malignant breast tumors.

Materials and Methods

The local Institutional Review Board approved this prospective single-institution study (EK 297/2007) and retrospective data analysis. The research was performed in accordance with relevant guidelines/regulations and informed consent was obtained from all patients prior to MRI of the breast.

Patients

Between 01/2011 and 12/2011, 117 patients with abnormal mammograms or ultrasound studies, ie, asymmetric density, architectural distortion, breast mass, or microcalcifications (BI-RADS 0, 4, or 5), underwent breast MRI with a standardized study protocol. Of these, 53 consecutive patients who fulfilled the following predefined inclusion criteria were retrospectively evaluated: histopathologically verified primary malignant breast lesion visible on MRI and no diagnostic or therapeutic intervention prior to the MRI examination. One patient was excluded due to technical failure of the DWI sequence, resulting in a study population of 52 (mean age 50.1 years, SD 13.3, range 26–82).

Imaging and Postprocessing

All patients underwent MRI at 3T (Tim Trio, Siemens, Erlangen, Germany) in the prone position. A four-channel breast coil (InVivo, Orlando, FL) was used. In premenopausal women, MRI was performed in the second week of the menstrual cycle.[2]

All patients underwent multiparametric MRI of the breast, including a T_2w sequence, a precontrast diffusion-weighted imaging sequence, and a dynamic contrast-enhanced (0.1 mmol/kg body weight Gd-DOTA, Dotarem, Guerbet, France) T_1w sequence.

For DWI, an axial, three-acquisition direction, trace diffusion-weighted, double-refocused, single-shot echo-planar imaging (EPI) sequence with short tau inversion recovery (STIR) fat-suppression

was used (repetition time / echo time / inversion time [TR/TE/TI] 13700/83/220 msec; field of view [FOV] 340 × 117 mm; 40 slices; matrix 192 × 64 [50% oversampling]; two averages; b-values 50 and 850 s/mm^2; bandwidth 1446 Hz/pixel; 3:19 min; phase-encoding direction anterior-to-posterior; frequency-encoding direction right-to-left; reconstructed resolution 1.8 × 1.8 × 3.5 mm).

Synthetic images with calculated b-values of 1000, 1200, 1400, 1600, 1800, and 2000 s/mm^2 were created by a monoexponential decay model, using the open-source DICOM-software HOROS,[20] with the ADCmap plugin[21] (Fig. 1).

Image Assessment and Data Analysis

For each patient, the slice in which the lesion of interest showed the largest diameter was used to create a single image for each synthetic b-value, as well as for the original image at b = 850 s/mm^2. In patients with more than one malignant lesion (n = 4), the largest lesion was selected as the lesion of interest.

Out of these images, an image set displaying all the different b-values was created for each patient.
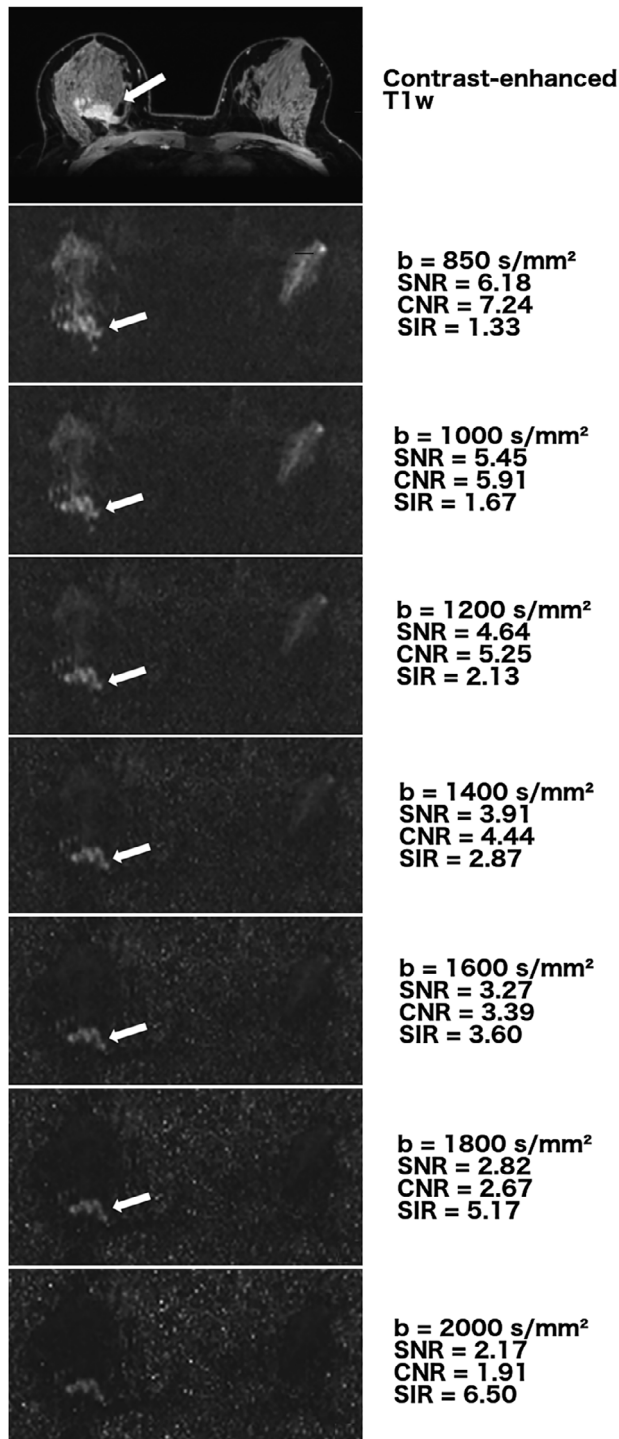
Four radiologists with different experience levels in breast imaging independently read the image collages: R1 (H.B.), 8 years of experience, with a special focus on breast DWI; R2 (P.B.), 15 years of experience; R3 (G.W.), 6 years of experience; and R4 (S.P.), 3 years of experience.

Each reader rated the general image quality and lesion visibility of every b-value image in each patient, using a visual grading characteristics (VGC) score of 1–5, with 5 being the best grade. In addition, each reader for each patient chose one b-value as their preferred, as well as the lowest acceptable and the highest acceptable b-value, over the range of b-values tested, to provide a diagnostic image.

R1 also read the T_1w images of the examined breasts for the amount of fibroglandular tissue (FGT) according to the BI-RADS lexicon and performed signal intensity (SI) measurements by placing round, 2D regions of interest (ROIs) into the visually determined, most hyperintense portion of the lesion of interest (SI_{Lesion}), in the normal breast tissue of the contralateral breast (SI_{Tissue}) if normal breast tissue was visible on the DWI images (n = 44), and in the air between the breasts ($SI_{Background}$) to calculate relative SNR, contrast-to-noise ratios (CNRs), and SI-Ratio (SIR) (Fig. 2). Relative SNR was calculated using the formula $SNR = \frac{SI_{Lesion}}{SI_{Background}}$. Relative CNR was calculated using the formula $CNR = \frac{SI_{Lesion} - SI_{Tissue}}{SD_{Background}}$. Relative SIR was calculated using the formula $SIR = \frac{SI_{Lesion}}{SI_{Tissue}}$. In cases with no measurable background parenchyma, only relative SNR was calculated. R1 repeated both the visual grading reading, as well as the signal measurements 1 month after the previous readings, for the evaluation of intrareader agreement. Lesion size was determined as the maximum diameter of the lesion of interest in the axial plane, measured in the contrast-enhanced T_1w series.

Statistical Analysis

Statistical analysis was performed using SPSS 19.0 (IBM, Armonk, NY) and MedCalc 12 (MedCalc Software, Ostend, Belgium). All calculations were performed on a per-lesion basis. Nominal data were presented using absolute frequencies and percentages. Differences in image quality and lesion visibility were calculated from the average results of all four readers. After testing for normal distribution, ordinal

Contrast-enhanced T1w

b = 850 s/mm²
SNR = 6.18
CNR = 7.24
SIR = 1.33

b = 1000 s/mm²
SNR = 5.45
CNR = 5.91
SIR = 1.67

b = 1200 s/mm²
SNR = 4.64
CNR = 5.25
SIR = 2.13

b = 1400 s/mm²
SNR = 3.91
CNR = 4.44
SIR = 2.87

b = 1600 s/mm²
SNR = 3.27
CNR = 3.39
SIR = 3.60

b = 1800 s/mm²
SNR = 2.82
CNR = 2.67
SIR = 5.17

b = 2000 s/mm²
SNR = 2.17
CNR = 1.91
SIR = 6.50

FIGURE 1: Contrast-enhanced T_1w (top image) and diffusion-weighted images of the same patient (55-year-old female with FGT type D and grade 2 invasive lobular cancer in the right breast [white arrow]) at different calculated b-values as displayed next to the image, and the corresponding relative SNR, CNR, and SIR. With increasing b-values, the nondiffusion-restricted background tissue is suppressed, while the restricted tumor retains its high signal intensity, increasing visibility.

and metric data were presented using median and interquartile ranges or mean and standard deviation. The grading scores for the different b-values, relative SNR, CNR, and SIR were compared using the Friedman test. In case of significant results, post-hoc analysis was performed
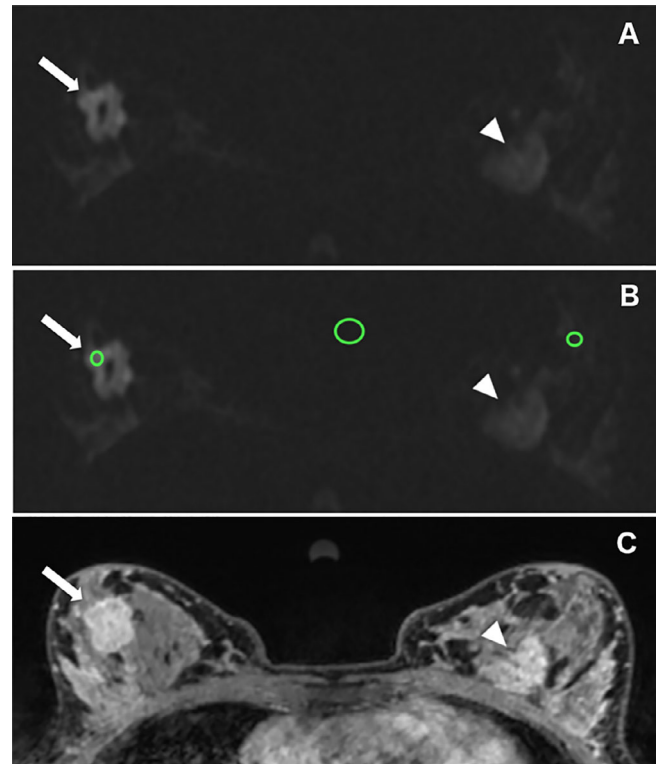
FIGURE 2: A 39-year-old female with grade 3 invasive ductal cancer in the right breast (arrow). Diffusion-weighted image at b = 850 s/mm² without (a) and with (b) the regions of interest (ROIs) used to calculate relative SNR, CNR, and SIR. Round/oval ROIs were placed inside the lesion of interest (right ROI), the air between the breasts (middle ROI), and the healthy breast tissue of the contralateral breast (left ROI). (c) The corresponding contrast-enhanced T_1w image. The lesion in the left breast (arrowhead) is a large fibroadenoma.

using pair-by-pair Wilcoxon signed-rank tests. Subgroup analysis for lesion visibility and preferred b-value was also performed in the different FGT types and between low (types A and B) and high breast FGT proportion (types C and D). Due to the low number of included patients with FGT type A (n = 2), no subgroup analysis could be performed for this FGT type. Interreader agreement was evaluated using intraclass correlation (ICC) and Fleiss κ, whereas intrareader agreement was evaluated using ICC and Cohen's κ. $P \leq 0.05$ was considered a significant result.

Results

The distribution of FGT types was: type A (n = 2), type B (n = 19), type C (n = 19), and type D (n = 12).

Mean lesion size was 31.4 mm (range 7–106). The included types of breast cancers were: 44 invasive ductal carcinomas (IDC, 84.6%), five pure ductal carcinoma in situ (DCIS, 9.6%), two invasive lobular carcinomas (ILC, 3.8%), and one invasive papillary carcinoma (IPC, 1.9%).

Signal Intensity Measurements

Relative SNR and relative CNR showed a continuous decrease with increasing b-values (Fig. 1), with significant differences between each of the b-values ($P < 0.001$). In

TABLE 1. Relative Signal Ratios Calculated From the Quantitative Signal Measurements in Tumor, Normal Breast Tissue, and Background Air

| b-value	SNR ± SD	CNR ± SD	SIR ± SD
850	16.4 ± 7.6	39.4 ± 23.4	3.7 ± 1.6
1000	14.1 ± 6.5	31.5 ± 18.6	4.2 ± 1.9
1200	11.7 ± 5.5	20.6 ± 12.2	4.9 ± 2.2
1400	9.8 ± 4.9	14.1 ± 8.5	5.9 ± 2.8
1600	8.0 ± 4.1	9.9 ± 6.1	7.0 ± 3.7
1800	6.4 ± 3.5	6.8 ± 4.4	8.3 ± 4.6
2000	5.1 ± 3.1	4.7 ± 3.2	9.9 ± 5.6

SNR, signal-to-noise ratio; SD, standard deviation; CNR, contrast-to-noise ratio; SIR, signal-intensity ratio. b-values are displayed in s/mm^2.

contrast, relative SIR showed a continuous increase with increasing b-values, with significant differences between each of the b-values ($P < 0.001$). Detailed results are displayed in Table 1 and Fig. 3.

Image Quality and Lesion Visibility

In the combined results, the image quality was rated significantly better in the images with b-values of 1400 s/mm^2
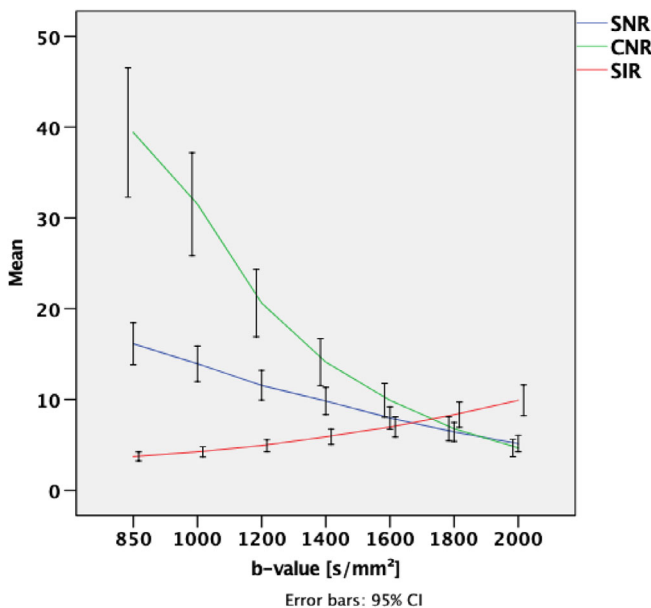
FIGURE 3: Line graph displaying mean relative SNR, CNR, and SIR between the lesions, normal breast tissue, and the air between the breasts at different b-values. While relative SNR and CNR are shown to decrease as b-values increase, relative SIR increases, reflecting the faster signal decrease of nondiffusion-restricted background tissue compared with the diffusion-restricted tumor. The error bars represent the 95% confidence intervals. B-values are displayed in s/mm^2.

(mean rank: 4.84), 1600 (4.79), and 1800 (4.49) than those with other b-values.

Lesion visibility was rated best in the images with b-values of 1200 s/mm^2 (mean rank: 3.94), 1400 (4.84), 1600 (4.79), and 1800 (4.49). An image example with the corresponding mean scores for each b-value is displayed in Fig. 4.

Preferred and Acceptable b-value

The distribution of the preferred and acceptable b-values chosen by the different readers is displayed in Fig. 5. Combining the results of all readers (Table 2), the images with a b-value of 1600 s/mm^2 were most commonly selected as the preferred b-value ($n = 65$, 31.3%), followed by 1400 ($n = 55$, 26.4%) and 1200 ($n = 41$, 19.7%).

Results Stratified by FGT type

As in the overall results, the preferred b-value was mostly between b = 1200–1600 s/mm^2 in the FGT B and C groups, while there was a slight shift to higher b-values in the FGT D group (Table 3). Lesion visibility was rated best between 1200–1600 s/mm^2 in the FGT B and C groups, while the best ratings were given between 1400–1800 s/mm^2 in the FGT D group (Fig. 6).

When comparing low to high FGT types, the preferred b-value was mostly between b = 1200–1600 s/mm^2 in the low FGT group and between 1400–1600 s/mm^2 in the high FGT group, while lesion visibility was rated best at b = 1200–1600 s/mm^2 in both subgroups (Table 3).
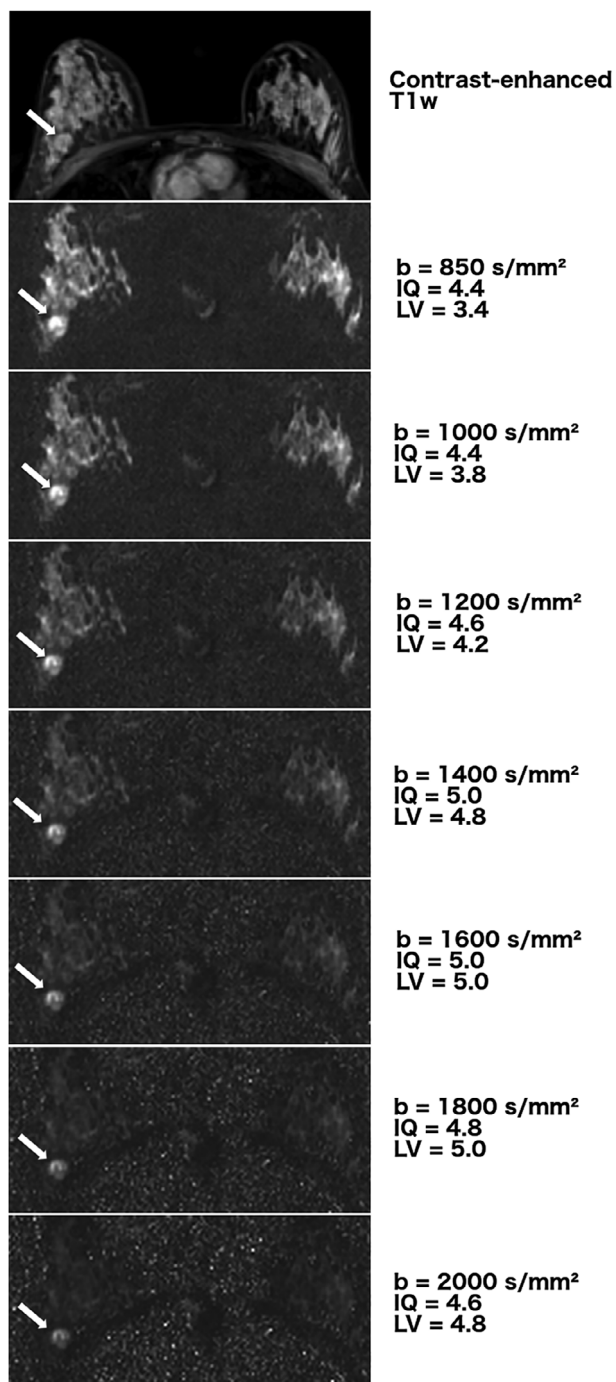
Reproducibility

Interreader agreement was moderate concerning image quality (ICC: 0.50–0.67) and moderate to high concerning lesion visibility (ICC: 0.70–0.93). Agreement was poor concerning the highest ($\kappa = 0.446$, $P < 0.001$) and lowest ($\kappa = 0.175$, $P < 0.001$) acceptable b-value, while no significant result could be produced concerning the overall preferred b-value ($\kappa = 0.032$, $P = 0.259$).

Intrareader agreement was generally good concerning image quality (ICC 0.832–0.846) except for the b = 850 and b = 2000 images, and moderate to excellent concerning lesion visibility (ICC 0.460–0.937). Agreement was moderate concerning the highest ($\kappa = 0.549$, $P < 0.001$) and lowest ($\kappa = 0.659$, $P < 0.001$) preferred b-value, and poor concerning the preferred b-value ($\kappa = 0.188$, $P = 0.004$).

Discussion

Our results show that images from synthetically increased b-values provide better lesion visibility and image quality than acquired images from routinely acquired lower b-values in DWI of the breast. Synthetic b-values of 1200–1800 s/mm^2 performed best regarding image quality, lesion visibility, and preferred b-value. Although higher synthetic b-values increase

Contrast-enhanced T1w

b = 850 s/mm²
IQ = 4.4
LV = 3.4

b = 1000 s/mm²
IQ = 4.4
LV = 3.8

b = 1200 s/mm²
IQ = 4.6
LV = 4.2

b = 1400 s/mm²
IQ = 5.0
LV = 4.8

b = 1600 s/mm²
IQ = 5.0
LV = 5.0

b = 1800 s/mm²
IQ = 4.8
LV = 5.0

b = 2000 s/mm²
IQ = 4.6
LV = 4.8

FIGURE 4: Contrast-enhanced T$_1$w (top image) and diffusion-weighted images of the same patient (27-year-old female with FGT type C and grade 3 invasive ductal cancer in the right breast [white arrow]) at different calculated b-values as displayed next to the image, and the corresponding mean scores from all readers for image quality (IQ) and lesion visibility (LV). The lesion is hardly visible on the contrast-enhanced image due to strong background parenchymal enhancement. IQ and LV increase with increasing b-values up to 1400–1800 s/mm², but are lower at b = 2000 s/mm².

background noise, these may be beneficial in patients with a higher portion of fibroglandular tissue. Reproducibility was moderate to good regarding image quality and lesion visibility, but poor concerning the preferred b-value of the readers,

which we interpret as an indicator for a range of preferred b-values rather than a specific value outperforming all others.

In theory, increasing b-values should lead to increasing background suppression and thus better lesion visibility. Accordingly, image quality and lesion visibility were rated best at intermediate to high b-values between 1200–1800 s/mm² and were significantly better than in the acquired image at b = 850 s/mm². In these images, the signal intensity of the background tissue was already fading significantly, allowing for a better visibility of the target lesion, while the background noise was not yet high enough to hinder lesion visibility. In addition, imaging artifacts such as wraparound artifacts were less visible with increasing b-values, which may have contributed to the more favorable results. Different b-values for breast DWI have been compared by O'Flynn et al; however, in their study only images from b-values of 1500 and 2000 s/mm² were calculated and these performed equally in terms of image quality.[18] Lesion visibility and image quality were rated best at intermediate b-values (1300 and 1600 s/mm²) in a study on cervical cancer,[22] while in the prostate, optimal b-values were reported to range between 1500–2500 s/mm²,[15] and 2000–3000, respectively.[17]

When looking at the subjectively preferred and the lowest and highest acceptable b-values, over the range of b-values tested, to provide a diagnostic image, in most cases, the lowest acceptable b-value was the original image (b = 850 s/mm²), while the highest acceptable b-value was 2000 s/mm². On the other hand, the preferred b-values were usually intermediate b-values, with a b-value of 1600 s/mm² most commonly selected, while the original image and the image at b = 2000 s/mm² were only rarely chosen. Thus, even while the original image was deemed diagnostic in about half of the cases, images from intermediate calculated b-values were preferred in most cases, again highlighting their superiority compared with the acquired and lower b-value images.

Dense breasts, ie, breasts with a high proportion of fibroglandular tissue, pose a particular challenge for breast cancer screening, since tumors are less conspicuous inside dense breasts and breast density poses an independent risk factor for the development of breast cancer.[23] Thus, women with high breast density would benefit particularly from the increasing background tissue suppression at high b-values. When stratified by FGT type, preferred b-value and best lesion visibility were reported at 1200–1600 s/mm² at FGT types B and C, while the best ratings at FGT type D were given when using b-values of 1400 to 1800 s/mm². This result again is in concordance with the theoretical background: in breasts with a small proportion of fibroglandular tissue, the tissue around the lesion is mostly comprised of fat, which is suppressed at the image acquisition (in the case of our study, by using an inversion recovery sequence), already providing a high lesion-to-background contrast in lower to intermediate b-value images. This contrast decreases at higher
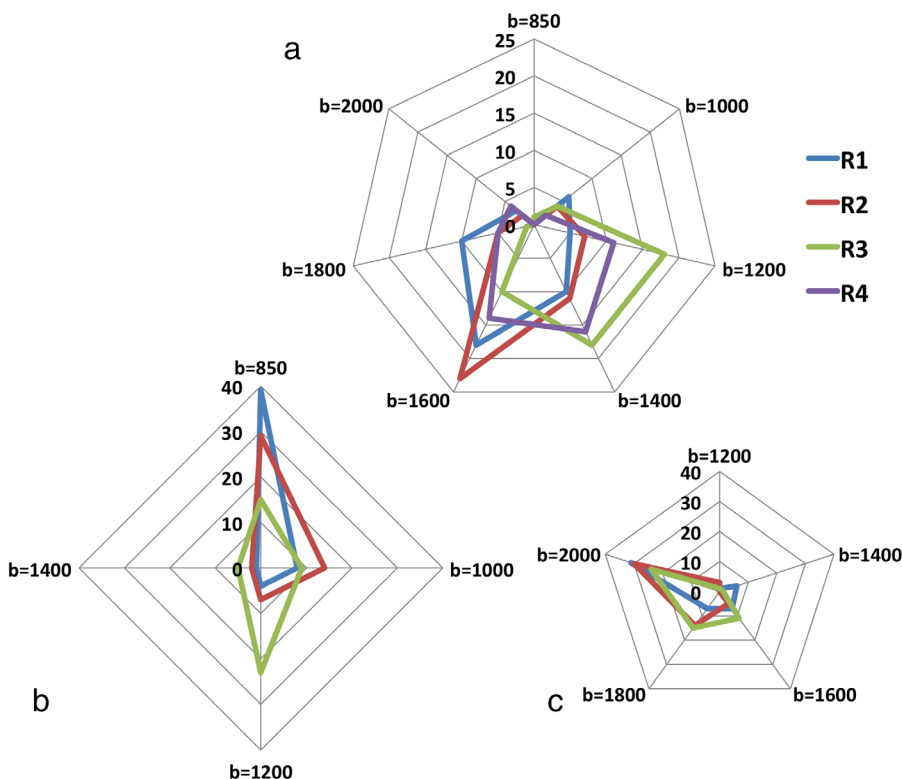
FIGURE 5: Radar charts displaying the number of mentions for preferred (a), lowest acceptable (b), and highest acceptable b-value (c) by readers 1–4 (R1-4). Images obtained with moderately increased b-values were most commonly chosen as the preferred b-value. B-values are displayed in s/mm^2.

b-values due to the signal loss of the lesion and the increase of background noise. On the other hand, in breasts with more fibroglandular tissue, this tissue is not completely suppressed in the lower b-value images, leading to a reduced lesion visibility. In higher b-value images, the normal fibroglandular tissue loses more signal than the diffusion restricted cancerous tumor, leading to better visibility.

As in theory, relative SNR and CNR should decrease at increasing b-values, while SIR, representing tumor-to-tissue contrast, will increase. Accordingly, the results of this study, as well as those of a phantom study published in 2011,[10]

show that this is also true for calculated b-values: tissue SI will decrease heavily with increasing b-values; diffusion-restricted, water-containing tumors such as most breast cancers will lose less signal; and background noise will increase. Similar results using calculated b-values have been reported, eg, in cervical cancer.[22]

As for every method, reproducibility of the results is an important measure of quality. In the case of this study, inter- and intrareader agreement was generally moderate to good concerning lesion visibility and image quality. While, to our knowledge, no comparable data are available for breast

TABLE 2. Combined Results of the Qualitative Readings by All Four Readers

b	Preferred	%	Lowest acceptable	%	Highest acceptable	%
850	1	0.5%	83	53.2%	0	0%
1000	16	7.7%	31	19.9%	0	0%
1200	41	19.7%	34	21.8%	5	3.2%
1400	55	26.4%	8	5.1%	7	4.5%
1600	65	31.3%	0	0%	23	14.7%
1800	21	10.1%	0	0%	36	23.1%
2000	9	4.3%	0	0%	85	54.5%

The absolute numbers displayed are the numbers of mentions for preferred, lowest acceptable, and highest acceptable b-value. B-values are displayed in s/mm^2.

TABLE 3. Mean Ranks for Lesion Visibility by b-Value and Fibroglandular Tissue (FGT) Type According to Friedman Test

|	FGT B $n = 19$	FGT C $n = 19$	FGT D $n = 12$	low FGT $n = 12$	high FGT $n = 31$
b = 850	2.97	2.74	2.04	3.00	2.47
b = 1000	3.26	3.89	2.88	3.36	3.50
b = 1200	**4.74**	**4.92**	3.96	**4.81**	**4.55**
b = 1400	**5.47**	**5.45**	**5.04**	**5.48**	**5.29**
b = 1600	**5.08**	**4.97**	**5.50**	**5.05**	**5.18**
b = 1800	4.13	3.82	5.13	4.05	4.32
b = 2000	2.34	2.21	3.46	2.26	2.69

Mean ranks above a cutoff of 4.5 are displayed in bold. A shift to higher b-values can be seen in breasts with FGT type D. B-values are displayed in s/mm^2.

tumors, these results are similar to those reported by Moribata et al, who found good agreement for lesion conspicuity using calculated b-values in cervical cancer.[22] The agreement was, however, poor concerning acceptable and preferred b-values. Since visibility and image quality were rated comparably well at b-values of 1200–1800 s/mm^2, the readers had 3–4 similarly good images to choose their favorite from, reducing the corresponding agreement. This indicates a range of preferred b-values rather than a specific value outperforming all others, while still supporting the fact that intermediate to high synthetic b-values are superior to the original image at a lower b-value.

This study has some limitations. First, no measurements with actually increased b-values were performed, so we were not able to compare the quantitative and qualitative results of the synthetic images to images physically obtained at higher b-values. However, the aim of this study was to prove whether calculated b-values provided an advantage over normal breast DWI, without the additional costs and scan time of acquired high b-value images. Second, we included only patients with known malignant breast tumors, so we were not able to provide information on the diagnostic accuracy of DWI with synthetic b-values for the diagnosis of breast cancer. It has been reported, however, that the visibility of benign lesions is much worse on DWI, a finding that must be considered beneficial in clinical practice.[24] Third, we used a single-shot EPI DWI sequence with STIR fat suppression. Different kinds of DWI sequences with alternative fat suppression techniques may provide different visual impressions and may therefore lead to different results concerning image quality and preferred b-values. Fourth, no healthy background tissue could be seen on DWI in some cases with FGT type B, due either to already high background suppression on the original images at b = 850 s/mm^2 or due to artifacts, so no CNR and SIR could be calculated for these lesions. Fifth, since the patients in this study were not recruited from a screening population, the average lesion size was rather high, which may limit the generalizability of the study results on screening populations.

In conclusion, DWI is a robust, reliable, and fast MRI sequence that has the potential to fulfill the need for an unenhanced technique for breast cancer imaging. Therefore, the optimization of this technique is mandatory and synthetically increased b-values, ideally at 1200–1800 s/mm^2, are one step towards reaching this goal. They provide better lesion visibility, image quality, and lesion-to-tissue contrast than acquired images at b-values commonly used in the breast, while the disadvantages of performing DWI at such high b-values may be avoided. Further prospective clinical studies should be performed to confirm the usefulness of this method.
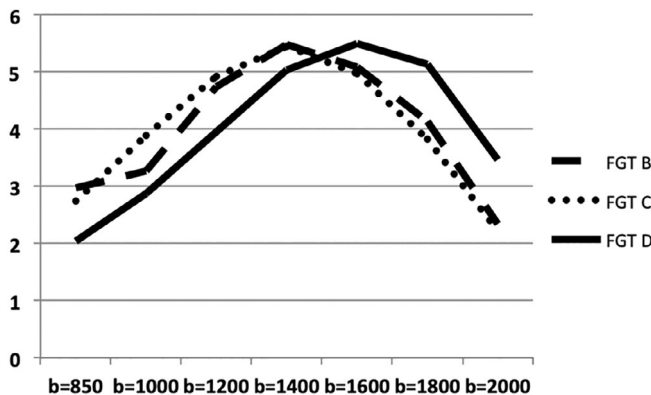
FIGURE 6: Line graph displaying the mean ranks for lesion visibility by b-value and FGT type according to the Friedman test. FGT type A was excluded from the analysis since only two cases with this FGT type were found in the study population. A shift to better lesion visibility at higher b-values can be seen in patients with FGT type D.

Acknowledgment

References

1. Monticciolo DL, Newell MS, Moy L, Niell B, Monsees B, Sickles EA. Breast cancer screening in women at higher-than-average risk: Recommendations from the ACR. J Am Coll Radiol 2018;15(3 Pt A):408–414.

2. Sardanelli F, Boetes C, Borisch B, et al. Magnetic resonance imaging of the breast: Recommendations from the EUSOMA working group. Eur J Cancer 2010;46:1296–1316.

3. Mann RM, Balleyguier C, Baltzer PA, et al. Breast MRI: EUSOBI recommendations for women's information. Eur Radiol 2015;25:3669–3678.

4. Saslow D, Boetes C, Burke W, et al. American Cancer Society guidelines for breast screening with MRI as an adjunct to mammography. CA Cancer J Clin 2007;57:75–89.

5. Ramalho J, Semelka RC. Gadolinium-based contrast agent accumulation and toxicity: An update. 2016;37:1192–1198.

6. EMA's final opinion confirms restrictions on use of linear gadolinium agents in body scans. EMA/457616/2017 (online resource).

7. Bogner W, Pinker-Domenig K, Bickel H, et al. Readout-segmented echo-planar imaging improves the diagnostic performance of diffusion-weighted MR breast examinations at 3.0 T. Radiology 2012;263:64–76.

8. Spick C, Bickel H, Pinker K, et al. Diffusion-weighted MRI of breast lesions: A prospective clinical investigation of the quantitative imaging biomarker characteristics of reproducibility, repeatability, and diagnostic accuracy. NMR Biomed 2016;29:1445–1453.

9. Clauser P, Marcon M, Maieron M, Zuiani C, Bazzocchi M, Baltzer PA. Is there a systematic bias of apparent diffusion coefficient (ADC) measurements of the breast if measured on different workstations? An inter- and intra-reader agreement study. Eur Radiol 2016;26:2291–2296.

10. Blackledge MD, Leach MO, Collins DJ, Koh DM. Computed diffusion-weighted MR imaging may improve tumor detection. Radiology 2011; 261:573–581.

11. Bogner W, Gruber S, Pinker K, et al. Diffusion-weighted MR for differentiation of breast lesions at 3.0 T: How does selection of diffusion protocols affect diagnosis? Radiology 2009;253:341–351.

12. Maas MC, Futterer JJ, Scheenen TW. Quantitative evaluation of computed high B value diffusion-weighted magnetic resonance imaging of the prostate. Invest Radiol 2013;48:779–786.

13. Grant KB, Agarwal HK, Shih JH, et al. Comparison of calculated and acquired high b value diffusion-weighted imaging in prostate cancer. Abdom Imaging 2015;40:578–586.

14. Bittencourt LK, Attenberger UI, Lima D, et al. Feasibility study of computed vs measured high b-value (1400 s/mm(2)) diffusion-weighted MR images of the prostate. World Radiol 2014;6:374–380.

15. Rosenkrantz AB, Parikh N, Kierans AS, et al. Prostate cancer detection using computed very high b-value diffusion-weighted imaging: How high should we go? Acad Radiol 2016;23:704–711.

16. Ueno Y, Takahashi S, Ohno Y, et al. Computed diffusion-weighted MRI for prostate cancer detection: The influence of the combinations of b-values. Br J Radiol 2015;88:20140738.

17. Vural M, Ertas G, Onay A, Acar O. Conspicuity of peripheral zone prostate cancer on computed diffusion-weighted imaging: Comparison of cDWI1500, cDWI2000, and cDWI3000. Biomed Res Int 2014;2014: 768291.

18. O'Flynn EA, Blackledge M, Collins D, et al. Evaluating the diagnostic sensitivity of computed diffusion-weighted MR imaging in the detection of breast cancer. J Magn Reson Imaging 2016;44:130–137.

19. Park JH, Yun B. Comparison of the diagnostic performance of synthetic versus acquired high b-value (1500 s/mm(2)) diffusion-weighted MRI in women with breast cancers. J Magn Reson Imaging 2018;49:857–863.

20. Horos. Free DICOM Medical Image Viewer. Available at: https:// horosproject.org Accessed May 2, 2019.

21. Hargreaves B. ADC map Plugin. Available at: https://horosproject.org/ horos-content/plugins/horos/ADCMap/html/ Accessed May 2, 2019.

22. Moribata Y, Kido A, Fujimoto K, et al. Feasibility of computed diffusion weighted imaging and optimization of b-value in cervical cancer. Magn Reson Med Sci 2017;16:66–72.

23. Harvey JA, Bovbjerg VE. Quantitative assessment of mammographic breast density: Relationship with breast cancer risk. Radiology 2004; 230:29–41.

24. Baltzer PA, Benndorf M, Dietzel M, Gajda M, Camara O, Kaiser WA. Sensitivity and specificity of unenhanced MR mammography (DWI combined with T2-weighted TSE imaging, ueMRM) for the differentiation of mass lesions. Eur Radiol 2010;20:1101–1110.